Title
Rational Design of a GFP-Based Fluorogenic Caspase Reporter for Imaging Apoptosis In Vivo

Journal
Cell Chemical Biology, 23(7)

ISSN
2451-9456

Authors
To, Tsz-Leung
Schepis, Antonino
Ruiz-González, Rubén
et al.

Publication Date
2016-07-01

DOI
10.1016/j.chembiol.2016.06.007

Peer reviewed

HHS Public Access

Author manuscript

Cell Chem Biol. Author manuscript; available in PMC 2017 January 21.

Published in final edited form as:

Cell Chem Biol. 2016 July 21; 23(7): 875–882. doi:10.1016/j.chembiol.2016.06.007.

Rational design of a GFP-based fluorogenic caspase reporter for imaging apoptosis *in vivo*

Tsz-Leung To[1,2], **Antonino Schepis**[2], **Rubén Ruiz-González**[1,2,3], **Qiang Zhang**[1,2], **Dan Yu**[1,2], **Zhiqiang Dong**[4], **Shaun R. Coughlin**[2], and **Xiaokun Shu**[1,2,*]

[1]Department of Pharmaceutical Chemistry, University of California – San Francisco, San Francisco, California, USA

[2]Cardiovascular Research Institute, University of California – San Francisco, San Francisco, California, USA

[3]Institut Químic de Sarrià, Universitat Ramon Llull, Via Augusta 390, 08017 Barcelona, Spain

[4]College of Life Sciences and Technology, Huazhong Agricultural University, Wuhan 430070, China

Summary

Fluorescence resonance energy transfer-based executioner caspase reporters using GFP are important tools for imaging apoptosis. While these reporters are useful in imaging apoptosis in cultured cells, their *in vivo* application has been handicapped by poor signal to noise. Here we report design and characterization of a GFP-based fluorogenic protease reporter, dubbed "ZipGFP". ZipGFP-based TEV protease reporter increased fluorescence 10-fold after activation by protease. A ZipGFP-based executioner caspase reporter visualized apoptosis in live zebrafish embryos with spatiotemporal resolution. Thus, the ZipGFP-based caspase reporter may be useful for monitoring apoptosis during animal development and for designing reporters of proteases beyond the executioner caspases.

eTOC Blurb

A fluorogenic protease reporter is developed by "zipping up" each fragment of split GFP in a manner that prevents their associate and fluorophore formation until release by specific proteolytic cleavage. The large signal enables imaging protease activity *in vivo*.

*To whom correspondence should be addressed. xiaokun.shu@ucsf.edu.

SUPPLEMENTAL INFORMATION

Supplemental Information includes Supplemental Experimental Procedures, 5 figures, 1 table and 10 movies and can be found with this article online.

AUTHOR CONTRIBUTIONS

X.S., S.R.C. initiated the project. X.S., T.-L.T designed the reporters. S.R.C., A.S. designed the experiments of zebrafish. T.-L.T., A.S., R.R., Q.Z., D.Y., Z.D. performed the experiments. X.S., T.-L.T. wrote the manuscript. All the authors contributed to the final draft.

COMPETING FINANCIAL INTERESTS

None declared.

Introduction

Förster resonance energy transfer (FRET)-based reporters using GFP are valuable tools in dissecting signaling pathways in living cells. Further understanding of molecular and cell biology requires investigation of cell signaling in living animals. However, in vivo use of FRET reporters is difficult for two main reasons (Kardash et al., 2011). First, the signal of FRET reporters is weak due to small fluorescence change of the donor and acceptor fluorophores. Secondly, fluorescence imaging of living animals is challenging because of tissue autofluorescence, cell heterogeneity and rapid shape and position changes. It is thus not surprising that use of FRET-based executioner caspase reporters in animals is limited (Campbell and Okamoto, 2013; Takemoto, 2003; Takemoto et al., 2007; Yamaguchi et al., 2011).

To overcome limitations of FRET-based executioner caspase reporters, we sought to design a GFP-based fluorogenic protease reporter that achieves several-fold fluorescence increase upon caspase activation. Very recently an infrared fluorogenic caspase reporter (iCasper) based on an infrared fluorescent protein (mIFP) was reported for imaging apoptosis in *Drosophila* (To et al., 2015). However, the bacterial phytochrome-based iCasper requires the cofactor biliverdin, which seems to be limiting in *Drosophila* and zebrafish (Yu et al., 2015). Although expression of heme oxygenase, which converts heme into biliverdin, overcomes this problem, a GFP-based fluorogenic reporter would be preferred since its fluorescence requires no cofactor in animals. Two GFP-based fluorogenic reporters, CA-GFP (Nicholls et al., 2011) and VC3AI (Zhang et al., 2013), have been used to image apoptosis in cultured cells. However, neither has been shown to detect apoptosis in animals such as zebrafish. Here we report the rational design of a GFP-based fluorogenic caspase reporter and its application to imaging apoptosis in the zebrafish embryo with spatiotemporal resolution.

Results and Discussion

Design of a protease reporter by caging GFP with mIFP

To design a GFP-based fluorogenic protease reporter, we modified the self-assembling split GFP so that its self-assembly is regulated by protease activity. GFP contains 11 β strands (Movie S1) (Ormö et al., 1996; Yang et al., 1996). One part of split GFP contains ten β strands (β1–10); the other part contains the 11th β strand (β11) (Cabantous et al., 2005). β1–10 contains three amino acids that form the chromophore (Tsien, 2009; 1998); whereas β11 contains the highly conserved Glu222 that catalyzes the chromophore maturation (Sniegowski, 2005). It has been shown that β11 rapidly binds to β1–10, and the green fluorescence develops within several tens of minutes (Cabantous et al., 2005). The crystal structure of GFP suggests a compact fit of β1–10 and β11, which presumably provides structural basis of the high binding affinity between the two parts (Movie S2). Based on this, we sought to prevent β11 binding to β1–10 by inserting β11 – a short peptide (16-residue) – into another protein in a manner that β11 could be hidden until made available by proteolysis.

To achieve this, we first used iProtease (the protein scaffold of iCasper) as a vehicle to cage β11 rather than as a fluorogenic reporter (Figure S1a). We inserted β11 between the PAS

and GAF domains of iProtease together with a TEV protease cleavage sequence (TevS) at a location previously suggested to be constrained until released by protease (Figure S1a) (To et al., 2015). The length of the insert plus TevS was 23 amino acids. Because insertions of > 11-residues at this site led to potentially decreased constraint based on appearance of weak infrared fluorescence of the iProtease reporter in the absence of the protease activity, we truncated the PAS domain so that β11 would likely be tightened or distorted. We made four constructs with various truncations of the PAS domain (Figure S1a). In addition, we used heterodimerizing coiled coils (E5 and K5) (De Crescenzo et al., 2003) to lock the PAS and GAF domains together. In the original iProtease design, the self-assembling split GFP was used to lock the PAS and GAF domains together. We next co-expressed the β11-mIFP and β1–10 in HEK293 cells (and mCherry as a reference), with or without the TEV protease (Figure S1b, c). However, we observed constitutive fluorescence without TEV-dependence. We hypothesized that this might be due to β1–10 binding to β11 before the translation or folding of the PAS domain and/or that β11 was not sufficiently constrained in the fully folded β11-mIFP.

To solve this problem, we decided to occlude the binding cavity of β1–10 so that it would not accommodate β11, with the occlusion being released by protease activity. We flanked the N and C-terminus of β1–10 with the heterodimerizing E5 and K5 coiled coils (Figure S1b), such that the leucine zipper–like E5/K5 coiled coils might block or “zip” the binding cavity and prevent β11 binding. Indeed the new design obtained ~ 5-fold fluorescence increase upon TEV protease cleavage (Figure S1d). However, we noticed punctate structures of the green fluorescence, when employing β11-mIFP with truncations to Cys18 and Ile23, both in the absence and presence of TEV protease. The number of punctate structures was significantly reduced for the β11-mIFP with truncations to Gly27 and Ile29. We considered further truncating the PAS domain to possibly reduce this potential aggregation problem and increase the signal gain to > 5-fold. However, Ile29 is already at the knot region of mIFP (Figure S1a, Movie S3) and further truncations would be expected to either prevent protease cleaving or block β11 from binding to β1–10 after protease cleavage by pulling β11 into the knot region. Therefore, the mIFP caging approach was abandoned, but the principle of caging both β11 and β1–10 was applied and turned out to be important (see below).

Design of a protease reporter by zipping GFP with coiled coils

In order to solve the aggregation problem and to further increase the signal, we decided to simply flank β11 with E5 and K5 since the coiled coils appear to successfully block β1–10. Based on this new design, E5/K5 heterodimer (with protease cleavage sequence) “zips” both β11 and β1–10 in order to prevent self-assembly of the split GFP (Figure 1a). Upon protease cleavage, both β11 and β1–10 are “unzipped”, which enables self-assembly and leads to fluorescence increase. We named this reporter ZipGFP. As a proof of concept, we designed a TEV protease reporter by inserting TEV cleavage sequence into ZipGFP (both the “zipped” β11 and β1–10). This ZipGFP-based TEV reporter achieved 10-fold fluorescence increase upon TEV cleavage in HEK293 cells with no punctate structures of the green fluorescence (Figure 1b, c). The fluorescence quantum yield of the reassembled ZipGFP was determined to be 0.25 (Supplemental Experimental Procedures). Zipping either β11 or β1–10 alone led to bright fluorescence even in the absence of TEV protease and the fluorescence did not

increase upon protease cleavage (Figure 1b). Thus, zipping of both β11 and β1–10 was required to adequately prevent reconstitution of split GFP in this system.

We next measured kinetics of ZipGFP-based protease reporter to determine its temporal resolution. First we separately purified two parts of ZipGFP in the presence of TEV protease. Then we mixed the cleaved ZipGFP and monitored green fluorescence over time. The green fluorescence increased over time with time to half-maximal fluorescence ($T_{1/2}$) of ~40 minutes (Figure 1d, e), which is similar to the previously reported kinetics for split GFP self-assembly (Cabantous et al., 2005). We also measured kinetics of ZipGFP in cells with a rapamycin-activatable TEV system, in which the two parts of split TEV are fused to FKBP and Frb (Gray et al., 2010; Wehr et al., 2006). Addition of rapamycin induces strong interaction between FKBP and Frb, which leads to reconstitution of split TEV. We co-expressed ZipGFP, mCherry and the rapamycin-activatable TEV system in HEK293 cells and monitored green and red fluorescence over time upon addition of rapamycin, which revealed $T_{1/2}$ ~ 100 minutes (Figure S2, Movie S4).

ZipGFP caspase reporter detects apoptosis in mammalian cells

To design a ZipGFP-based caspase reporter for imaging apoptosis, we inserted the consensus cleavage sequence (DEVD) of caspase 3 into both parts of ZipGFP. The well characterized signaling pathways of apoptosis are composed of extrinsic and intrinsic pathways, both of which lead to activation of the executioner caspases that include caspase 3 (Crawford and Wells, 2011). Detection of activated caspase 3 using antibody has been proved to be useful in identifying apoptotic cells in animals including zebrafish (Sorrells et al., 2013). And the conserved cleavage sequence (DEVD) of caspase 3 has been used in the previous caspase reporters(Ding et al., 2015; Nicholls et al., 2011; Takemoto, 2003; To et al., 2015; Zhang et al., 2013).

We expressed ZipGFP in the human glioblastoma LN229 cells. Upon addition of staurosporine, which induces apoptosis by activating caspase 3(Tee and Proud, 2001), ZipGFP's green fluorescence increased significantly in cells treated with staurosporine (Figure 2a, Movie S5), whereas the fluorescence signal of ZipGFP has no or little change in cells without treatment with staurosporine (Movie S6). To account for a potential increase of the reporter's concentration with time after transient transfection, we co-expressed mCherry. The ratio of green fluorescence to mCherry's red fluorescence revealed a 5–10 fold increase of ZipGFP's fluorescence upon apoptosis. Activation of caspase 3 in ZipGFP fluorescing cells was confirmed using a commercially available small molecule active-site modifier for far-red fluorescent imaging of caspase 3 activity (Figure 2b). And the onset of apoptosis in single cells as detected by ZipGFP varied between 2 and 5 hours after addition of staurosporine (Figure 2c), consistent with previous results (Albeck et al., 2008). Additionally, replacing the caspase cleavage site in ZipGFP β11 with TevS abolished the fluorescence increase upon apoptosis (Figure S3), suggesting that the increased fluorescence requires caspase cleavage.

We next compared ZipGFP to a previous GFP-based fluorogenic caspase reporter CA-GFP. CA-GFP was reported to show 45-fold fluorescence increase after caspase activation in bacteria and 3-fold increase in mammalian cells upon staurosporine-induced apoptosis

(Nicholls et al., 2011). However, we observed less than 1-fold fluorescence increase after normalization by a co-expressed red fluorescent protein in LN229 cells upon addition of staurosporine (Figure 2d). We also compared ZipGFP to VC3AI, another previous GFP-based caspase reporter. Green fluorescence of VC3AI normalized to co-expressed mCherry in LN229 cells showed 2–6 fold fluorescence increase upon addition of staurosporine (Figure 2e), which is slightly smaller than ZipGFP. Together, these data suggest that the newly designed ZipGFP is one of the best choices in genetically encoded caspase detection in mammalian cells.

It should be pointed out that compared to iCasper, the fluorescence increase of ZipGFP is slower after triggering apoptosis. This is consistent with the in vitro $T_{1/2}$ of ZipGFP ~ 40 min. being significantly slower than that of iCasper (<10 seconds). The different kinetics is likely due to different mechanisms of fluorescence development: for iCasper, the chromophore is an endogenous molecule and rapidly binds to the activated reporter, and thus quickly becomes fluorescent (To et al., 2015). On the other hand, the chromophore of GFP is formed from three amino acids in a reaction that requires tens of minutes (Tsien, 1998). Nevertheless, our results demonstrated that ZipGFP develops fluorescence sufficiently fast to visualize caspase 3 activity and apoptosis in cultured mammalian cells.

ZipGFP visualizes caspase activity and apoptosis in live zebrafish

To determine whether the fluorescence signal and the temporal resolution of ZipGFP are sufficient for imaging apoptosis in animals, we expressed the ZipGFP-based caspase reporter in zebrafish. Zebrafish was chosen based on optical transparency and its importance as a model organism among vertebrate animals (Grunwald and Eisen, 2002). We injected mRNA encoding ZipGFP caspase reporter and mCherry linked via a T2A site into the embryo at the one-cell stage (Online Methods). T2A is a “self-cleaving” peptide used in co-expression of multiple genes (Szymczak et al., 2004).

We exposed the zebrafish embryo at the 50% epiboly stage (i.e. the blastoderm covers 50% of the entire distance between the animal and vegetal poles) to 100 μg/ml cycloheximide (Figure 3a), which was previously shown to induce apoptosis in the early zebrafish embryo (Negron and Lockshin, 2004). The embryo continued to develop with epiboly continuing for 2 hours after exposure to cycloheximide (Figure 3b, Movie S7), but cell movement became arrested at 2 hours and cells started to retract at 3 hours. During this time, the embryo showed bright mCherry fluorescence, indicating that the reporter was well expressed, but green fluorescence was absent or dim, suggesting that the caspase was inactive in the embryo. However, by 4 hours, green fluorescence became obvious in a few cells, and after 5 – 6 hours of treatment, many cells showed strong green fluorescence, suggesting caspase activation and apoptosis. Indeed, many of these cells were also fragmented or showed a round shape, consistent with cellular morphological change during apoptosis. In the absence of cycloheximide treatment, embryonic development continued normally with evident somite formation as expected; red fluorescence was easily detected but green fluorescence was negligible, consistent with little apoptosis occurring during this early stage of development (Figure 3c). Caspase activation using antibody staining against the cleaved caspase 3 was confirmed in the zebrafish embryo treated with cycloheximide (Figure S4),

and the observed effects of cycloheximide treatment on the zebrafish embryo are consistent with a previous demonstration of cycloheximide-induced apoptosis in this setting (Negron and Lockshin, 2004).

After demonstrating that the ZipGFP caspase reporter could be used to image cycloheximide-induced apoptosis in early zebrafish embryo during gastrulation stage, we next demonstrated that this system could be used to visualize spatiotemporal dynamics of apoptosis during normal embryo development after gastrulation stage. We again expressed the ZipGFP caspase reporter (and mCherry) in zebrafish embryos by injection of mRNA at the one-cell stage. Time-lapse imaging of the head was started at 24 hours post fertilization (hpf) (Figure 3d). At this time, little green fluorescence was observed (Figure 3d, Movie S8). 10 hours later, green fluorescence was detected in a couple of cells. After 15 – 20 hours, more cells showed strong green fluorescence. By contrast, mCherry fluorescence was weak and decreased over time (Movie S8), presumably because its mRNA injected at the one-cell stage was degraded over time and/or diluted as development progressed. Green, presumed apoptotic cells were distributed around the developing retina and the forebrain. In particular, time-lapse imaging first detected green fluorescence on the rostral aspect of the forebrain. The number of green cells increased over time and they appeared to form clusters. These cells appeared to have neuron-like long extensions or processes (Figure 3d, inset). Z-section imaging indicated that many of them appeared to be located on the outer layer of the forebrain and the retina (Movie S9). Caspase activation in the brain region of zebrafish embryo at 48 hpf was confirmed using antibody staining against the cleaved caspase 3, which overlapped with ZipGFP fluorescence (Figure S5). Imaging of the trunk region of the zebrafish embryo also revealed green cells around dorsal part of the somites and in the tail bud (Figure 3e). Some of them extended into the intersomitic regions (inset of Figure 4e, Movie S10).

The spatial pattern of ZipGFP fluorescence we observed in the zebrafish embryo is consistent with a previous study based on TUNEL staining that showed clusters of apoptotic cells in the developing brain as well as in the trunk including the tail bud (Cole, 2001). While TUNEL staining lacks temporal resolution, the temporal pattern revealed by ZipGFP indicated that apoptosis first occurred at the rostral part of the forebrain (Movie S6). It has been suggested that apoptosis provides a mechanism of removing neurons that failed to form appropriate connections during early neural circuit formation. Although our data suggest that the apoptotic cells in the brain are morphologically like neurons, detailed studies will be required to identify the cell type(s) and to reveal the molecular mechanisms. For example, specific promoters may be used to express the ZipGFP caspase reporter in the neurons or other cell types in the transgenic zebrafish or zebrafish that express ZipGFP ubiquitously may be bred with existing lines that express fluorescent markers specifically in cell-types of interest. And genetic manipulation can be used to investigate specific mechanisms of apoptosis.

Significance

We have designed a fluorogenic protease reporter by “zipping” both parts of the self-assembling split GFP. ZipGFP-based protease reporter achieves ~10-fold fluorescence

increase upon proteolytic cleavage, which is significantly larger than FRET-based fluorescence change of the donor and acceptor fluorophores and is thus ideal in imaging apoptosis *in vivo*. We have demonstrated that ZipGFP-based executioner caspase reporter is able to visualize apoptosis in the living embryos of zebrafish, which is an important model vertebrate for understanding embryonic development (Grunwald and Eisen, 2002). ZipGFP caspase reporter will thus be an important tool in imaging apoptosis *in vivo*, which plays essential roles in animal development, maintenance of tissue homeostasis, and disease(Fuchs and Steller, 2011; Jacobson et al., 1997). It will be useful to dissect signaling networks that lead to apoptosis by hypothesis-driven studies as well as unbiased high throughput screening in live animals such as zebrafish. ZipGFP may be further used to design reporters of many other proteases, which are essential for many biological processes (Lopez-Otin and Bond, 2008). These fluorogenic reporters overcome the sensitivity limitation of FRET-based reporters and will be suitable for imaging protease activity in physiological environments.

EXPERIMENTAL PROCEDURES

DNA constructs

The details of all constructs in this study are listed in Table S1. All plasmid constructs were created by standard molecular biology techniques and confirmed by exhaustively sequencing the cloned fragments. DNA of VC3AI was synthesized with codon optimization for expression in mammalian cells.

Protein purification and characterization

The pBAD constructs used for protein expression in *E. coli* are listed in Table S1. Proteins were purified with the Ni-NTA purification system (Qiagen). Protein concentration was measured by the BCA method (Pierce).

Mammalian cell cultures

The HEK293T/17 (ATCC CRL-11268) and LN-229 (ATCC CRL-2611) were obtained from ATCC. Cells were passaged in Dulbecco's Modified Eagle medium (DMEM) supplemented with 10% Fetal Bovine Serum (FBS), nonessential amino acids, penicillin (100 units/mL) and streptomycin (100 μg/mL). All culture supplies were obtained from the UCSF Cell Culture Facility.

Confocal microscopy

For characterization of the protease reporters in cultured mammalian cells, transfected HEK293T/17 or LN-229 cells were imaged in 35 mm glass bottom microwell dishes on a Nikon Eclipse Ti inverted microscope equipped with a Yokogawa CSU-W1 confocal scanner unit (Andor), a digital CMOS camera ORCAFlash4.0 (Hamamatsu), a ASI MS-2000 XYZ automated stage (Applied Scientific Instrumentation) and a Nikon Plan Apo λ 20X air (N.A. 0.75) objective. Image acquisition was controlled by the NIS-Elements Ar Microscope Imaging Software (Nikon). Images were processed using NIS-Elements and ImageJ (NIH).

Characterization in cultured mammalian cells

HEK293T/17 cells transiently transfected with TEV reporter or TEV reporter + TEV were imaged in 35 mm glass bottom dishes ~24 hours after transfection. For time-lapse imaging of the Caspase-3 reporter during apoptosis, LN-229 cells at ~24 hours after transient transfection with the reporter were grown in 35 mm glass bottom dishes to ~90% confluence. Time-lapse microscopy was performed using the confocal microscope described above with the aid of an environmental control unit incubation chamber (InVivo Scientific), which was maintained at 37°C and 5% CO_2. To induce apoptosis, 1 μM of Staurosporine (STS) was added to cells in PBS.

Characterization in zebrafish embryos

Zebrafish was handled in compliance with local animal welfare regulations and were maintained according to standard protocols (http://zfin.org). The culture was conducted in conformity with UCSF IACUC and AAALAC guidelines. In order to make mRNA for injection, the plasmid pCS2+ ZipGFPT2a-mCherry was linearized with KpnI. *In vitro* transcription was performed using the mMachine mMessage Kit (Ambion). 100 pg of mRNA were injected at one cell stage.

Supplementary Material

Refer to Web version on PubMed Central for supplementary material.

Acknowledgments

This work was supported by National Institute of General Medical Sciences (NIGMS) R01 GM115399 (to X.S.), R01 HL054737 and R01 HL121387 (to S.R.C.), EMBO fellowship ref. 306–2015 (to R.R-G). We thank Dr. Binghui Li for sharing the coding sequence of VC3AI.

References

Albeck JG, Burke JM, Aldridge BB, Zhang M, Lauffenburger DA, Sorger PK. Quantitative analysis of pathways controlling extrinsic apoptosis in single cells. Mol Cell. 2008; 30:11–25. DOI: 10.1016/j.molcel.2008.02.012 [PubMed: 18406323]

Cabantous S, Terwilliger TC, Waldo GS. Protein tagging and detection with engineered self-assembling fragments of green fluorescent protein. Nat Biotechnol. 2005; 23:102–107. DOI: 10.1038/nbt1044 [PubMed: 15580262]

Campbell DS, Okamoto H. Local caspase activation interacts with Slit-Robo signaling to restrict axonal arborization. J Cell Biol. 2013; 203:657–672. DOI: 10.1007/400_2009_20 [PubMed: 24385488]

Cole L. Apoptosis in the Developing Zebrafish Embryo. Developmental biology. 2001; 240:123–142. DOI: 10.1006/dbio.2001.0432 [PubMed: 11784051]

Crawford ED, Wells JA. Caspase substrates and cellular remodeling. Annu Rev Biochem. 2011; 80:1055–1087. DOI: 10.1146/annurev-biochem-061809-121639 [PubMed: 21456965]

De Crescenzo G, Litowski JR, Hodges RS, O'Connor-McCourt MD. Real-Time Monitoring of the Interactions of Two-Stranded de NovoDesigned Coiled-Coils: Effect of Chain Length on the Kinetic and Thermodynamic Constants of Binding †. Biochemistry. 2003; 42:1754–1763. DOI: 10.1021/bi0268450 [PubMed: 12578390]

Ding Y, Li J, Enterina JR, Shen Y, Zhang I, Tewson PH, Mo GCH, Zhang J, Quinn AM, Hughes TE, Maysinger D, Alford SC, Zhang Y, Campbell RE. Ratiometric biosensors based on dimerization-

dependent fluorescent protein exchange. Nat Methods. 2015; 12:195–198. DOI: 10.1038/nmeth.3261 [PubMed: 25622108]

Fuchs Y, Steller H. Programmed Cell Death in Animal Development and Disease. Cell. 2011; 147:742–758. DOI: 10.1016/j.cell.2011.10.033 [PubMed: 22078876]

Gray DC, Mahrus S, Wells JA. Activation of specific apoptotic caspases with an engineered small-molecule-activated protease. Cell. 2010; 142:637–646. DOI: 10.1016/j.cell.2010.07.014 [PubMed: 20723762]

Grunwald DJ, Eisen JS. Headwaters of the zebrafish—emergence of a new model vertebrate. Nat Rev Genet. 2002; doi: 10.1038/nrg891

Jacobson MD, Weil M, Raff MC. Programmed cell death in animal development. Cell. 1997; 88:347–354. [PubMed: 9039261]

Kardash E, Bandemer J, Raz E. Imaging protein activity in live embryos using fluorescence resonance energy transfer biosensors. Nat Protoc. 2011; 6:1835–1846. DOI: 10.1038/nprot.2011.395 [PubMed: 22051797]

Lopez-Otin C, Bond JS. Proteases: Multifunctional Enzymes in Life and Disease. J Biol Chem. 2008; 283:30433–30437. DOI: 10.1074/jbc.R800035200 [PubMed: 18650443]

Negron JF, Lockshin RA. Activation of apoptosis and caspase-3 in zebrafish early gastrulae. Dev Dyn. 2004; 231:161–170. DOI: 10.1002/dvdy.20124 [PubMed: 15305296]

Nicholls SB, Chu J, Abbruzzese G, Tremblay KD, Hardy JA. Mechanism of a Genetically Encoded Dark-to-Bright Reporter for Caspase Activity. J Biol Chem. 2011; 286:24977–24986. DOI: 10.1074/jbc.M111.221648 [PubMed: 21558267]

Ormö M, Cubitt AB, Kallio K, Gross LA, Tsien RY, Remington SJ. Crystal structure of the Aequorea victoria green fluorescent protein. Science. 1996; 273:1392–1395. [PubMed: 8703075]

Sniegowski JA. Base Catalysis of Chromophore Formation in Arg96 and Glu222 Variants of Green Fluorescent Protein. J Biol Chem. 2005; 280:26248–26255. DOI: 10.1074/jbc.M412327200 [PubMed: 15888441]

Sorrells S, Toruno C, Stewart RA, Jette C. Analysis of Apoptosis in Zebrafish Embryos by Whole-mount Immunofluorescence to Detect Activated Caspase 3. JoVE. 2013; doi: 10.3791/51060

Szymczak AL, Workman CJ, Wang Y, Vignali KM, Dilioglou S, Vanin EF, Vignali DAA. Correction of multi-gene deficiency in vivo using a single “self-cleaving” 2A peptide-based retroviral vector. Nat Biotechnol. 2004; 22:589–594. DOI: 10.1038/nbt957 [PubMed: 15064769]

Takemoto K. Spatio-temporal activation of caspase revealed by indicator that is insensitive to environmental effects. J Cell Biol. 2003; 160:235–243. DOI: 10.1083/jcb.200207111 [PubMed: 12527749]

Takemoto K, Kuranaga E, Tonoki A, Nagai T, Miyawaki A, Miura M. Local initiation of caspase activation in Drosophila salivary gland programmed cell death in vivo. Proc Natl Acad Sci USA. 2007; 104:13367–13372. DOI: 10.1073/pnas.0702733104 [PubMed: 17679695]

Tee AR, Proud CG. Staurosporine inhibits phosphorylation of translational regulators linked to mTOR. Cell Death Differ. 2001; 8:841–849. DOI: 10.1038/sj.cdd.4400876 [PubMed: 11526437]

To TL, Piggott BJ, Makhijani K, Yu D, Jan YN, Shu X. Rationally designed fluorogenic protease reporter visualizes spatiotemporal dynamics of apoptosis in vivo. Proceedings of the National Academy of Sciences. 2015; 112:3338–3343. DOI: 10.1073/pnas.1502857112

Tsien RY. Constructing and exploiting the fluorescent protein paintbox (Nobel Lecture). Angew Chem Int Ed Engl. 2009; 48:5612–5626. DOI: 10.1002/anie.200901916 [PubMed: 19565590]

Tsien RY. The green fluorescent protein. Annu Rev Biochem. 1998; 67:509–544. DOI: 10.1146/annurev.biochem.67.1.509 [PubMed: 9759496]

Wehr MC, Laage R, Bolz U, Fischer TM, Grünewald S, Scheek S, Bach A, Nave KA, Rossner MJ. Monitoring regulated protein-protein interactions using split TEV. Nat Methods. 2006; 3:985–993. DOI: 10.1038/nmeth967 [PubMed: 17072307]

Yamaguchi Y, Shinotsuka N, Nonomura K, Takemoto K, Kuida K, Yosida H, Miura M. Live imaging of apoptosis in a novel transgenic mouse highlights its role in neural tube closure. J Cell Biol. 2011; 195:1047–1060. DOI: 10.1101/gad.1984410 [PubMed: 22162136]

Yang F, Moss LG, Phillips GN. The molecular structure of green fluorescent protein. Nat Biotechnol. 1996; 14:1246–1251. DOI: 10.1038/nbt1096-1246 [PubMed: 9631087]

Yu D, Baird MA, Allen JR, Howe ES, Klassen MP, Reade A, Makhijani K, Song Y, Liu S, Murthy Z, Zhang SQ, Weiner OD, Kornberg TB, Jan YN, Davidson MW, Shu X. a naturally monomeric infrared fluorescent protein for protein labeling. Nat Methods. 2015; 12:763–765. DOI: 10.1038/nmeth.3447 [PubMed: 26098020]

Zhang J, Wang X, Cui W, Wang W, Zhang H, Liu L, Zhang Z, Li Z, Ying G, Zhang N, Li B. Visualization of caspase-3-like activity in cells using a genetically encoded fluorescent biosensor activated by protein cleavage. Nature Communications. 2013; 4:2157.doi: 10.1038/ncomms3157

Highlights

- Split GFP is “zipped” or redesigned to sense protease activity
- ZipGFP-based caspase reporter detects apoptosis in human cells
- ZipGFP caspase reporter enables imaging physiological apoptosis in zebrafish

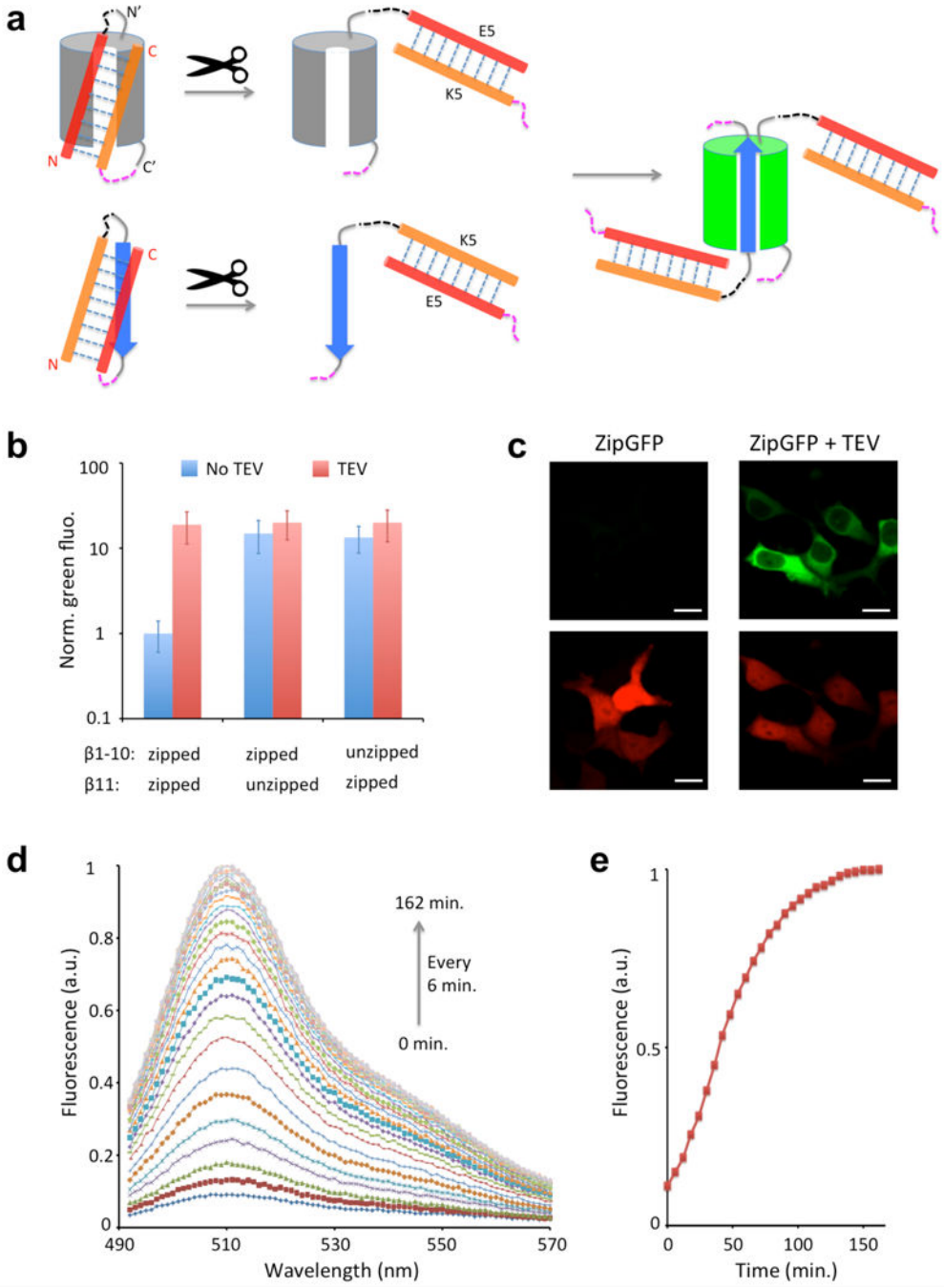

Figure 1. Rational design and characterization of a ZipGFP protease reporter

(**a**) Schematic diagram of ZipGFP. β1–10 (in gray) is flanked with E5 and K5 (in red and orange, respectively) at N and C-terminus, respectively. β11 (in blue) is flanked with K5 and E5 (in orange and red, respectively) at N and C-terminus, respectively. The protease cleavage sequence is shown in pink. (**b**) The green fluorescence normalized by co-expressed mCherry for unmodified (i.e. unzipped) or modified (i.e. zipped) β1–10 and β11 as in (**a**). (**c**) Fluorescence images of ZipGFP with TEV cleavage sequence expressed in HEK293 cells. Scale bar: 10μm. (**d**) Emission spectra of ZipGFP over time. The two parts of cleaved

ZipGFP were purified and mixed (β1–10: 2.7 μM; β11: 6.3 μM). The fluorescence spectra were then taken every 6 minutes. (**e**) The green fluorescence intensity over time after mixing of two cleaved parts of ZipGFP as in (d). The fluorescence intensity was calculated based on the emission spectra by integrating emission from 490 to 550 nm.

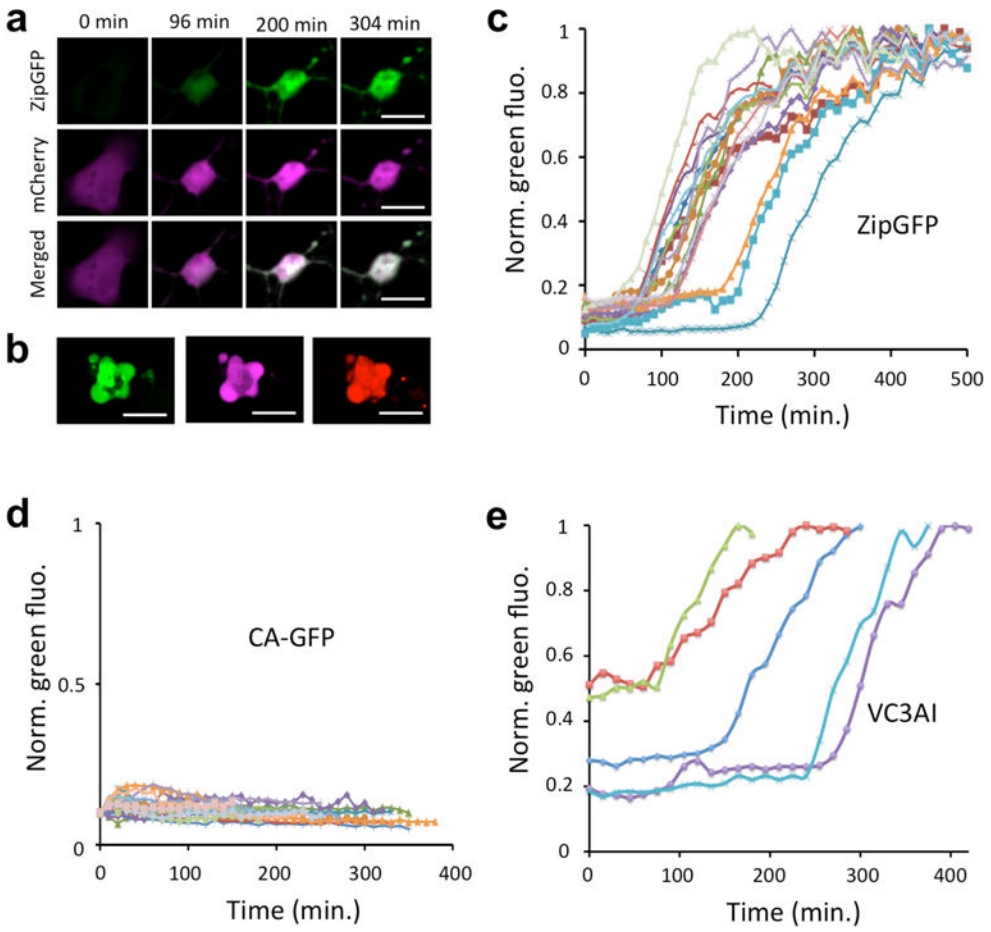

Figure 2. Characterization and comparison of ZipGFP caspase reporter in mammalian cells

(**a**) Time-lapse confocal images of human glioblastoma cells LN229 expressing ZipGFP caspase reporter upon treatment with 1μM staurosporin. See also Movie S4. mCherry was co-expressed. (**b**) Confocal image of the LN229 cell expressing ZipGFP caspase reporter and stained with caspase imaging agent FLICA after addition of staurosporine. Top: green fluorescence from GFP; middle: red fluorescence from co-expressed mCherry; bottom: far-red fluorescence from FLICA 660 caspase 3/7 reagent. (**c**) Normalized green fluorescence of LN229 cells expressing ZipGFP caspase reporter reveals 5 – 10 folds fluorescence increase and cell-to-cell heterogeneity of caspase activation upon addition of staurosporin. The green fluorescence was normalized by co-expressed mCherry red fluorescence based on confocal images of live cells after treatment with 1μM staurosporin, which were collected every 10 minutes. (**d**) Normalized green fluorescence of LN229 cells expressing CA-GFP caspase reporter reveals < 1 fold fluorescence increase upon addition of staurosporin. mLumin, a red fluorescent protein, was co-expressed and used to normalize the CA-GFP fluorescence. (**e**) Normalized green fluorescence of LN229 cells expressing VC3AI caspase reporter reveals 2 – 6 fold fluorescence increase upon addition of staurosporin. The red fluorescent protein mCherry was co-expressed and used to normalize the VC3AI fluorescence. Scale bars, 20 μm (a), 15 μm (b).

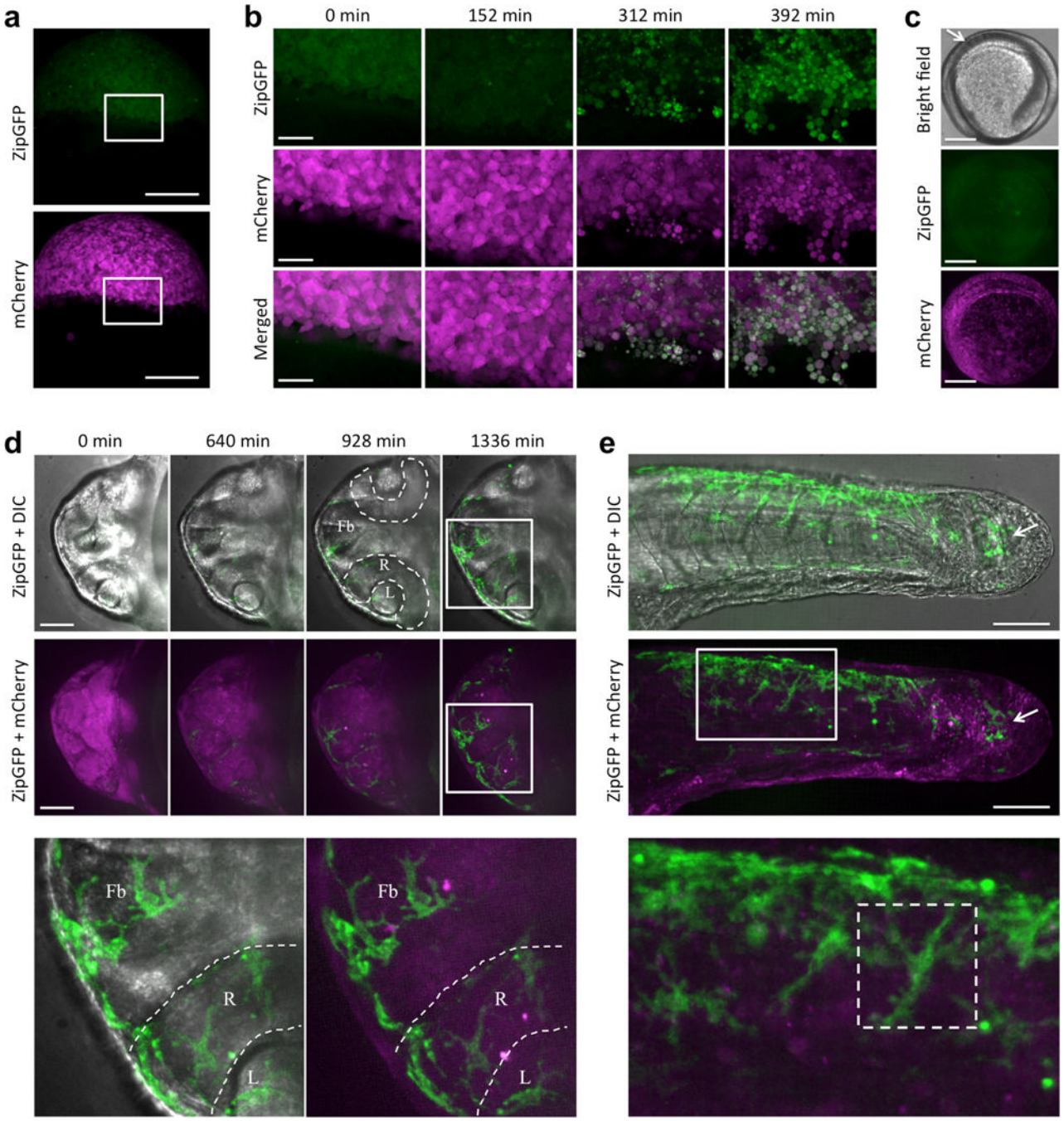

Figure 3. ZipGFP caspase reporter in imaging apoptosis in zebrafish

(**a**) Confocal images of the zebrafish embryo at the 50% epiboly stage expressing ZipGFP caspase reporter and mCherry. (**b**) Time-lapse fluorescence images of zebrafish embryo in the zoomed area in (**a**) after addition of cycloheximide. (**c**) Confocal images of the control zebrafish embryo (no addition of cyclohexide) expressing ZipGFP caspase reporter at 12 hpf. Arrow points to one of the somites. (**d**) Time-lapse images of the brain of the zebrafish embryo expressing ZipGFP caspase reporter and mCherry. Imaging started at 24 hpf (see Movie S6). Fb: forebrain; R: retina; L: lens. The dashed lines outline the retina. (**e**) Images

around the trunk of the zebrafish embryo expressing ZipGFP caspase reporter and mCherry at 48 hpf. Arrow points to the tail bud. Scale bar: 200 μm (**a**); 50 μm (**b**); 200 μm (**c**); 80 μm (**d, e**).